THE INFLUENCE OF CENTRE BOW LENGTH ON SLAMMING LOADS AND MOTIONS OF LARGE WAVE-PIERCING CATAMARANS

(DOI No: 10.3940/rina.ijme.2018.a1.451)

J R Shahraki, University of Tasmania, Australia, **G A Thomas**, University College London, United Kingdom and **M R Davis**, University of Tasmania, Australia

SUMMARY

The effect of various centre bow lengths on the motions and wave-induced slamming loads on wave-piercing catamarans is investigated. A 2.5 m hydroelastic segmented model was tested with three different centre bow lengths and towed in regular waves in a towing tank. Measurements were made of the model motions, slam loads and vertical bending moments in the model demi-hulls. The model experiments were carried out for a test condition equivalent to a wave height of 2.68 m and a speed of 20 knots at full scale. Bow accelerations and vertical bending moments due to slamming showed significant changes with the change in centre bow, the longest centre bow having the highest wave-induced loads and accelerations. The increased volume of displaced water which is constrained beneath the bow archways is identified as the reason for this increase in the slamming load. In contrast it was found that the length of centre bow has a relatively small effect on the heave and pitch motions in slamming conditions.

1. INTRODUCTION

1.1 WET DECK DESIGN APPROACHES FOR CATAMARANS

Wave-Piercing Catamarans (WPCs) with centre bows are becoming more widely used for their superior stability, large deck area for loading and unloading cars and trucks, high speeds and ability to avoid deck diving. Figure 1 shows a 112 m INCAT Tasmania wave-piercing catamaran with the centre bow.

Tunnel clearance, centre bow volume, reserve buoyancy and unprotected area of centre bow are key parameters of the WPC hull form. The unprotected area of centre bow, as shown in ……. is defined as the projected area of the centre bow which is visible from the side and is thus not constrained by the demi-hulls during slamming. The water displaced by bow entry is able to exit sideways above the demi-hull bows as the bow enters the water.

Figure 1. A photo of Mols-Linjen 112 m wave piercing catamaran with centre bow built by INCAT Tasmania (www.INCAT.com.au, 2017)

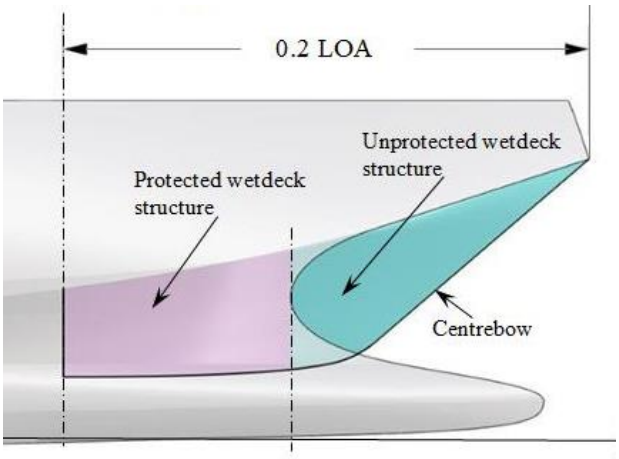

Figure 2. Fore section of an Incat wave-piercing catamaran, LOA = 112m showing the protected and unprotected structures at the bow section with approximately 20% of LOA (Swidan, 2016)

By examining the slamming mechanism from full-scale trials of WPCs (Thomas et al., 2003b, Jacobi et al., 2014), it was proposed that centre bow volume and tunnel clearance have a significant influence on seakeeping and slamming behaviour. These two parameters account for the crucial differences between the two common strategies taken by catamaran designers to reduce or avoid slamming. As depicted in Figure 2 the two approaches to decrease or avoid slamming are either using a large wet deck height or introducing a centre bow with significant reserve buoyancy above the calm water line. Too high a tunnel clearance could result in operational problems when loading and unloading, and too low a tunnel clearance could increase the risk of high slam loads.

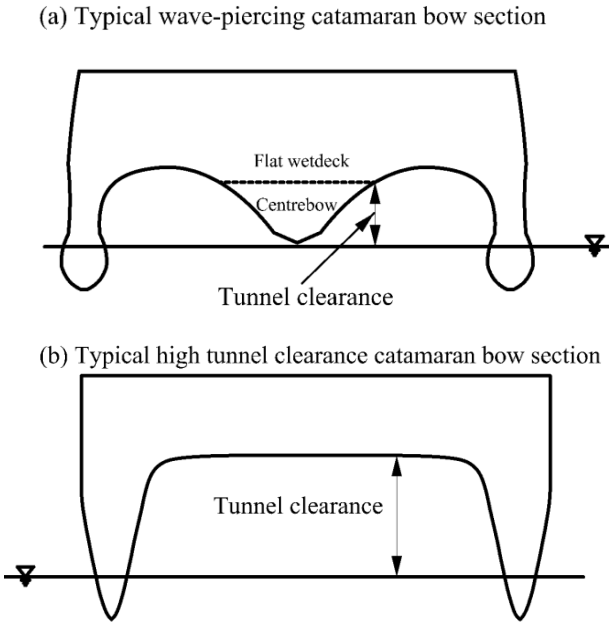

Figure 3. Typical bow profiles of WPCs and conventional catamarans. Narrow water-plane area of demi-hulls, low tunnel clearance and centre bow are the main characteristics of INCAT Tasmania large WPCs

In the case of the WPC configuration adopted by INCAT Tasmania, identification of the optimal configuration of hull form specifically focuses on the centre bow shape and the volume required to improve seakeeping, avoid deck diving and reduce slam loads. By keeping other hull parameters, such as tunnel clearance, constant, one of the major objectives of this work was to investigate the effect of changes in centre bow volume on slamming behaviour including vessel motions and wave-induced loads.

1.2 INVESTIGATION METHODS FOR EFFECT OF HULL FORM ON SLAMMING

Full-scale measurements are an important method for investigating slamming behaviour (Jacobi et al., 2014, Kapsenberg, 2011, Thomas et al., 2003a). However, there are several practical and analytical issues:

- Complicated instrumentation and measurement processes are involved in acquiring data during sea trials, which makes such experiments expensive and time consuming.
- The environmental factors cannot be controlled and so it is difficult to select the required seaway conditions.
- The measurement of the encountered waves is difficult and has significant uncertainties.
- It is difficult to collect pressure data on the hull as the owners/operators are reluctant to drill holes in the vessel hull.
- The key difficulty is to relate the structural response of the vessel to slam loads. A complicated process using a finite element model can be used to obtain a load case by a “reverse engineering” process (Amin et al., 2008).
- It is not possible to investigate the influence of variation of hull form on slam behaviour.

Model drop tests are a useful means for detailed pressure and flow observations on water entry sections. Swidan et al. (2017) conducted a series of three-dimensional controlled speed water impact tests to evaluate the slamming loads of a 3D WPC’s bow section using two interchangeable centre bows. However, the three-dimensional effect on slam peak pressures, loads and impact pulse timing has been investigated by Swidan et al. (2016) and Whelan (2004) and Davis and Whelan (2007), showing that simplifying the wetdeck slam phenomenon as a quasi-2D problem can be considered to be an invalid assumption for such complex hull forms. Therefore, application of the results of these tests and relevant two-dimensional theories is not a satisfactory method to investigate the complex vessel sections such as WPC bow sections.

An effective experimental alternative is model testing in a towing tank, where hydroelastic segmented model tests are necessary since the duration of slam loads and the period of whipping are similar and the loading of the ship structure by slamming wave impact is influenced by both the hydrodynamic transient and transient structural response. The results of these experiments can define slamming occurrence criteria and identify motions, slam loads and vertical bending moments (VBM) during slamming and the subsequent whipping vibrations (Lavroff et al., 2013).

Whilst the effect of bow flare shape and general body form for the seakeeping and slamming of monohulls has been investigated e.g. by Kapsenberg and Brizzolara (1999), Hermundstad and Moan (2005) and Bereznitski (2001), there is insufficient data available on the effects of catamaran hull form on seakeeping, slamming and structural loads. Ge et al. investigated wet-deck slamming of a high speed conventional catamaran using a three segment model (Ge et al., 2005). Dessi et al. recently designed and tested a hydroelastic segmented catamaran model measuring motions and slam loads (Dessi et al., 2016). However, the full 3D effect of hull form changes, in particular the effect of variation of bow geometry of WPC has not been investigated. In this paper hydroelastic segmented model experiments are used to investigate the effect of variation of centre bow length and volume.

1.3 FLEXURAL RIGIDITY AND VIBRATORY RESPONSE OF THE MODEL

In view of the 100 m length of the towing tank at the Australian Maritime College, which is 3.5 m wide and 1.4 m deep, an overall model of length of 2.5 m was selected to represent the 2500 tonnes, 112 m INCAT

Tasmania WPC, giving a scale ratio of 1/44.8. Following the approach adopted for an earlier hydroelastic segmented model (HSM01) of the 112 m INCAT vessel (Lavroff et al., 2013, Thomas et al., 2012, Thomas et al., 2010), the new variable geometry Hydroelastic Segmented Model (HSM02, as shown in Figure 4) was designed with each demi-hull split into three segments, the segment cuts being at 33% and 56% of the model length from the transom. The three segments of each demi-hull were connected using short, rectangular section, aluminium elastic links with strain gauges fitted to the upper and lower surfaces of each link (see Figure 5). The two strain gauges on each link were then connected in a single bridge circuit enabling direct measurement of the vertical bending moment in the link.

Figure 4 shows the fully assembled model in the wet dock of the towing tank. As can be seen the mid and aft segment demi-hulls are connected using two carbon-fibre box wet decks and there are two aluminium beams connecting the forward demi-hull segments demi-hulls to the centre bow.

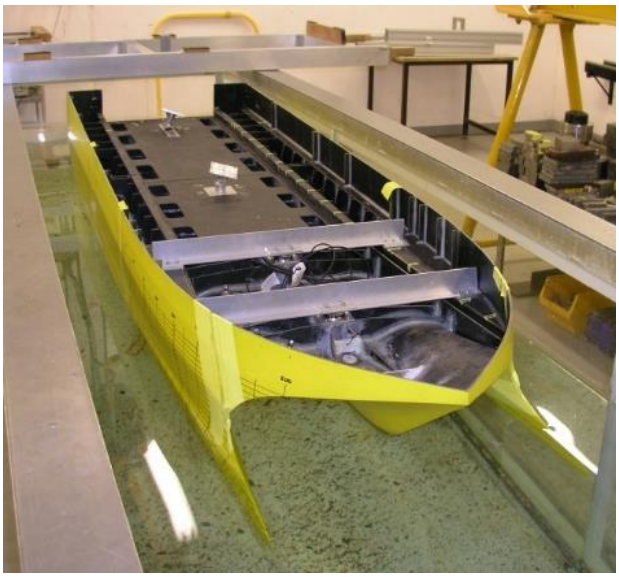

Figure 4: Hydroelastic model HSM02 representing an INCAT 112 m vessel in the wet dock of Australian Maritime College towing tank

The hydroelastic behavior of the model was adjusted to represent the full scale vessel with a first longitudinal mode whipping frequency of approximately 2.2 Hz (Matsubara, 2011). According to model scaling principles the modal frequencies are as given by

$$f_m = f_s \sqrt{\frac{L_s}{L_m}} \qquad (1)$$

where f_m and f_s are the model and full-scale frequencies respectively. The desired model wet modal frequency of the model is therefore 14.7 Hz. By assuming rigid segments in the model, the wet vibratory response is determined by the stiffness of the elastic links, the mass distribution of the model, the body form and the surrounding water. Figure 5 shows a drawing of one of the aluminium elastic links used in the model. Both ends of the elastic links were machined to fit inside the rectangular hollow backbone beams mounted within each hull segment with three aluminium bolts (two vertical and one horizontal). Using the method described by (Lavroff et al., 2007) for a three degree of freedom model, the appropriate dimensions of the elastic links (i.e. the dimensions of the square cross section and the length of the link) were obtained to give the required model stiffness.

Since the exact mass distribution of the model was not known before construction and since the segments were not totally rigid, exact prediction of the whipping frequency of the model was difficult. Therefore, impulse experiments were conducted with various elastic link dimensions so as to measure the whipping frequency directly, changing the stiffness by modifying link dimensions. The final frequency was achieved with a stiffer link than originally designed, having a square section of 15 mm and length 13 mm between the two ends. The nominal stiffness of the link based on its cross section and length was calculated to be 2271.6 Nm/rad and the average whipping frequency obtained in water at zero speed was 14.7 Hz which corresponded to 2.2 Hz at full-scale. The average damping ratio for the first few cycles was 0.01, which is similar to the damping ratio observed in full-scale anchor drop tests and in sea trials with severe slamming (Thomas et al., 2010, Thomas et al., 2008).

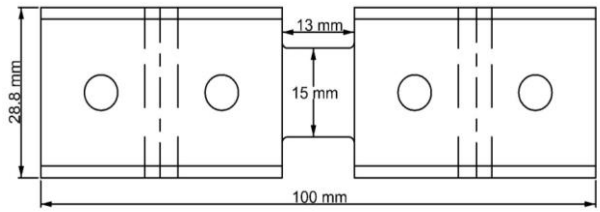

Figure 5: a schematic top view of an elastic link

To ensure rigidity of the connection between the segment links and the demihull segments, aluminium square hollow section backbone beams were build into the demi-hulls and attached to the carbon-fibre hulls at multiple frames. The aluminium square sections for the backbone beams were 32×32×1.6 mm in cross section and had lengths of 225 mm in the forward segment and 260 mm in the aft segment. As can be seen in Figure 6, the backbone beams were supported at least at three points by the transverse frames and bulkheads. Carbon-fibre longitudinal return decks were also assembled on top of the transverse frames to provide increased rigidity to the segments.

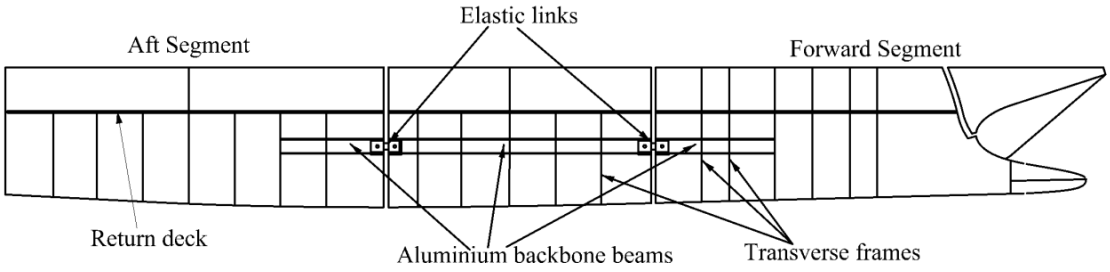

Figure 6: Backbone beams and the transverse frames arrangement in 2.5 m hydroelastic catamaran model HSM02

The model links were calibrated by static loading in both the upright and inverted positions and the calibration factors were averaged for hogging and sagging conditions. Calibration tests were carried out before and after the tank testing programme and only very small changes were observed, these being mainly due to deformation of soft sealing latex covering the small gaps between the hull segments.

2. DESIGN OF THE HYDROELASTIC SEGMENTED MODEL FOR TESTING VARIATIONS OF HULL FORM

The first INCAT Tasmania prototype wave-piercing catamaran was built and tested in 1983. Although following the characteristics of the early design, the geometry and size of the centre bow in INCAT WPCs have varied as these vessels have evolved. By reviewing the different designs adopted, as Figure 7 shows, the centre bow volume has increased in proportion to the vessel size, up to a vessel length of approximately 90 m.

For the recent larger vessels, the centre bow volume has decreased slightly in proportion to the overall hull, becoming approximately constant for vessels larger than 100 m in length. The centre bow is usually truncated at its largest sectional area within the forward third of the vessel overall length. The easiest and most effective way to alter centre bow volume without interfering too much with the bow shape and streamlining is to cut the centre bow volume from its aft end thus changing the centre bow length. The centre bow length is defined as the projected distance between the hull most forward point and the truncation of the centre bow. The Centre bow Length Ratio (CLR) is defined as Equation (2):

$$Centre\ bow\ Length\ Ratio\ (CLR) = \frac{Centre\ bow\ Length}{Demihull\ Length} \qquad (2)$$

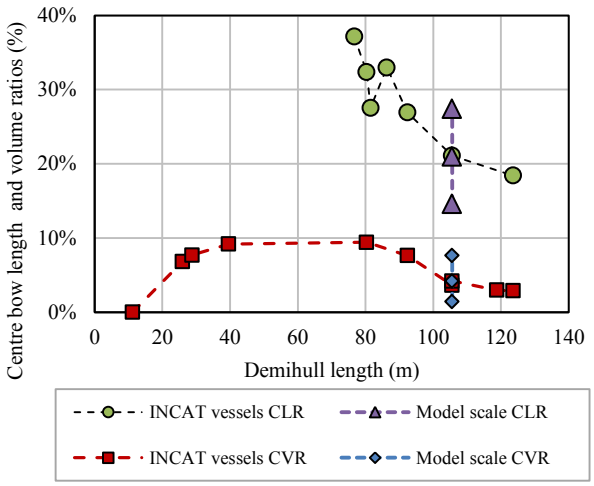

Figure 7: Centre bow length ratio (CLR) and centre bow volume ratio (CVR) of INCAT large wave-piercing catamarans and the ratio variations tested

As seen in Figure 7, the centre bow length ratio (CLR), has decreased from 37% to 18% as the vessel length has increased from 80 m to 130 m. The 2.5 m HSM02 is modelled on the INCAT Tasmania 112 m catamaran that has a 21% CLR and is referred to here as the parent centre bow.

Three different centre bow lengths were considered and the new centre bow lengths were created by removing a 6.72 m (150 mm model-scale) section from the aft end of the parent centre bow model to make a short centre bow and by extending the body lines of the parent centre bow 6.72 m by adding model centre bow segments under the wet deck to make the long centre bow. As seen in Figure 7 the CLR covered by this variation is 6.4% higher and lower than the parent design. Figure 7 illustrates how the added and removed sections create the three centre bow test lengths.

As shown in Figure 8, the centre bow volume is the volume of the centre bow bounded by the keel line of the centre bow and the flat horizontal main wet deck plane extended forward. The centre bow volume varied significantly between the three centre bow test lengths. The key characteristics of these three centre bow lengths are given in Table 1. The model total displacement volume was 0.027 m^3.

Table 1: Three centre bow lengths and volumes selected for experiments with the 2.5m WPC model HSM02

Model Name	Centre bow Length (m)	Centre bow Length Ratio (CLR)	Centre bow Volume (m^3)	Centre bow Volume Ratio (CVR)
Short Centre bow	0.348	14.6%	4.0696×10^{-4}	1.44%
Parent Centre bow	0.498	21%	11.8934×10^{-4}	4.22%
Long Centre bow	0.648	27.4%	21.5579×10^{-4}	7.64%

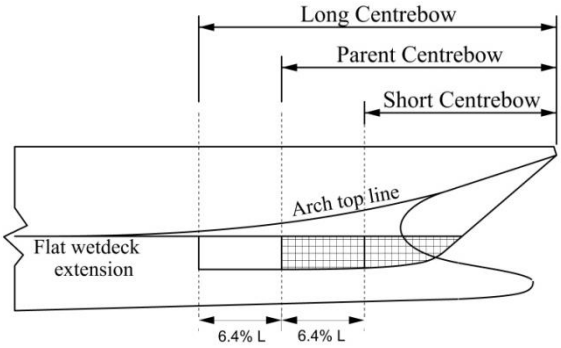

Figure 8: The creation of three centre bow lengths by adding and removing 150 mm pieces from the model parent centre bow truncation. The hatched area shows the parent centre bow volume

The centre bow Volume Ratio (CVR) is defined as,

$$Centre\ bow\ volume\ ratio\ (CVR) = \frac{Centre\ bow\ volume\ below\ the\ wet\ deck\ leve}{Total\ vessel\ displacement} \quad (3)$$

Figure 9 shows the final three centre bow lengths before painting. The extensions to the centre bows were attached to the hull section using three bolts and the gaps filled with plasticine to make the surface smooth and sealed. The weight of the extension pieces was 0.2 kg, but the total centre bow weight and centre of gravity remained constant by using counterweights. For HSM02 the centre bow and arch areas are isolated as a separate segment to capture the slamming loads.

Figure 9: Three centre bow length segments of HSM02 under construction. The short centre bow was achieved by cutting 150 mm from centre bow aft end and a separate segment was built to form the long centre bow.

As seen in Figure 9, the cuts were made in locations in the demi-hulls to include all the centre bow and archways and having minimum water flow disturbances. The centre bow segment extended at its outboard edges to a location where the hull cross section became vertical, the demi-hulls becoming broader below that edge. The centre bow segment was supported by two aluminium transverse beams to the demi-hulls and attached by two 6-degree of freedom load cells to measure the slam forces transmitted by the bow onto the demi-hulls.

3. EXPERIMENTAL PROCEDURE

The experiments were conducted in the Australian Maritime College (AMC) towing tank which incorporates a carriage that runs on rails positioned on the tank walls with a maximum speed of 4.5 m/s. The model was towed using a two post towing system, allowing the model to freely heave, pitch and roll. The average water temperature was 18°C, the average air temperature was 21°C and the density of the water was 998.85 kg/m^3 during the experiments.

The model was ballasted at level trim and the LCG of the model and each segment were measured by balancing the model. The pitch radius of gyration of the model was determined by using the Bifilar technique (Lloyd, 1989). Table 2 shows the model dimensions and parameters. As can be seen, the mass was increased slightly by 0.58 kg compared to the initial design value due to the addition of an extra motion sensor at the LCG.

During the tests, up to 32 channels of signals could be recorded via the data acquisition (DAQ) Card. The recorded channels for which data is presented here were: carriage speed, two LVDT signals on the tow posts to determine heave and pitch, a B&K 4370 piezoelectric accelerometer to measure the centre bow vertical acceleration, one static wave probe and two moving probes one in line with the model LCG and one in line with the model centre bow truncation, four strain gauge channels measuring VBMs at the segment joints and twelve channels recording the signals from the two 6 degree of freedom load cells on which the bow was mounted. The sampling rate was set to 5000 Hz for all the data channels. Figure 10 shows the model located underneath the carriage in AMC towing tank.

Table 2: HSM02 Model Particulars and Equivalent Full Scale Values

Item	Model scale	Full-scale
Scale factor	1/44.8	1
Length overall	2.5 m	112 m
Demihull length	2.35 m	105.6 m
Displacement	27.7 kg	25530 tonnes
LCG	0.941 m from transom	42.15 m from transom
Radius of gyration	0.67 m from LCG	30.16 m from LCG
Forward segment mass, LCG	8.37 kg, 1.804 m	-
Mid segment mass, LCG	7.57 kg, 1.298 m	-
Aft Segment mass, LCG	11.76 kg, 0.381 m	-
Trim	0 degrees	0 degrees
Fundamental structural modal frequency in calm water	14.7 Hz (measured)	2.2 Hz

Figure 10: The AMC towing tank carriage and the HSM02 in the water

The three centre bow configurations were tested at 1.53 m/s and 60 mm wave height, which correspond to 20 knots and 2.688 m of wave height at full-scale. Due to the complexity of the instrumentation and model set up for testing in different conditions, the main aim for the experiments was to obtain high quality results for a limited range of conditions. Regular waves were generated at encounter frequencies from 0.4 Hz to 1.1 Hz, with intervals of 0.5 Hz or 0.25 Hz. Better resolution of model motions and loads was achieved around the frequencies of peak motions by conducting tests at smaller frequency intervals. Selected runs were repeated multiple times to determine repeatability of the obtained results e.g. in peak motions.

4. MOTION RESULTS

Following ITTC guidelines (ITTC, 2014), motion results for seakeeping experiments are presented as non-dimensional response amplitude operators (RAOs), the heave RAO being the ratio of heave to wave height and the pitch RAO being the ratio of pitch value to maximum wave slope. Wave slopes for the longest waves were corrected for shallow water effects based on semi-empirical dispersion formula provided by (Fenton and McKee, 1990, Fenton, 1990). The motion RAOs are shown as functions of the non-dimensional encountered wave angular frequency (ω_e^*),

$$\omega_e^* = 2\pi \times f_e \times \sqrt{L/g} \qquad (4)$$

where L is the vessel overall length, g is the gravitational acceleration and f_e is the encountered wave frequency observed by the moving wave probes. Figure 11 shows the heave RAOs for the three centre bows. As expected, the heave response in high frequency waves is very small and in the long waves (low frequencies) the heave response RAO tends to one. There is a local maximum around $\omega_e^* = 3.7$. Slamming was visually observed in the mid-range of frequencies ($3.7 \leq \omega_e^* \leq 5.4$) for all the three centre bows. It was found that less than 1% standard error was observed in the non-dimensional heave values for three repeat runs.

The heave results show that for high and low frequencies, the results for the three centre bows are quite similar although in the frequency region of the local peak in RAO ($3.4 \leq \omega_e^* \leq 4$), the short centre bow has about a 13% higher heave motion than the long centre bow.

Figure 11 shows the pitch RAO with the three centre bows. As can be seen, the pitch RAO also tends to one at low frequency and reduces to zero at high frequency. The maximum pitch RAO occurs between $\omega_e^* = 3$ and 3.4 which is a slightly lower frequency than the frequency of maximum heave RAO. Similarly, less than 1% standard error was observed in the non-dimensional pitch values for three repeat runs.

The pitch motions show only small differences between the three centre bow lengths near to the frequencies of maximum pitch RAO. There is also a slight shift in the frequency of maximum pitch RAO between the three centre bow lengths, with the short centre bow having the smallest frequency for maximum pitch ($\omega_e^* = 3.14$). The small change in the frequency of the maximum magnitude of the RAOs appears to imply that the effect of a change in hydrodynamic stiffness is greater than any change in inertia forces in waves due to added mass effects. That is, the lesser volume in the short centre bow creates less pitch stiffness compared to the other two centre bows. For frequencies between $\omega_e^* = 3.7$ and $\omega_e^* = 5$ where severe wet deck slamming occurred during the runs, the pitch response of the short centre bow is on average 5% less than for the long centre bow. The reason for this will be discussed in more detail in the following sections when the slam loads are considered.

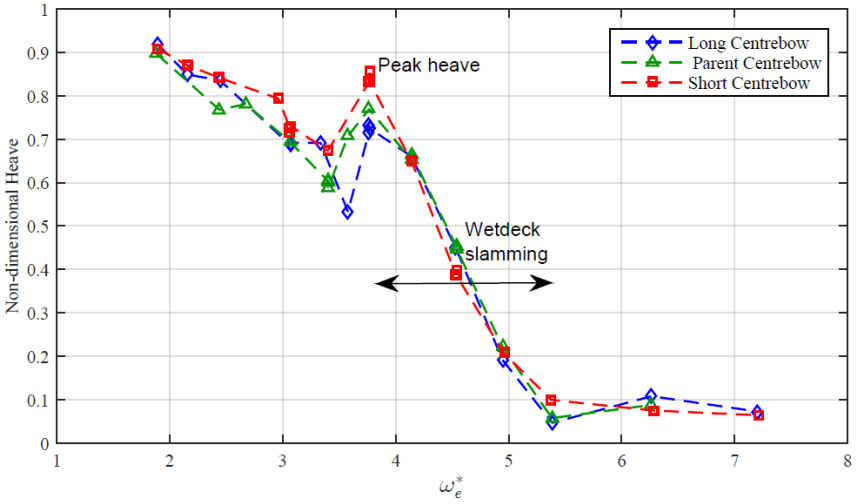

Figure 11: Non-dimensional heave response (RAO) for various centre bow lengths on HSM02 ($H_w = 60$ mm, speed=1.53 m/s)

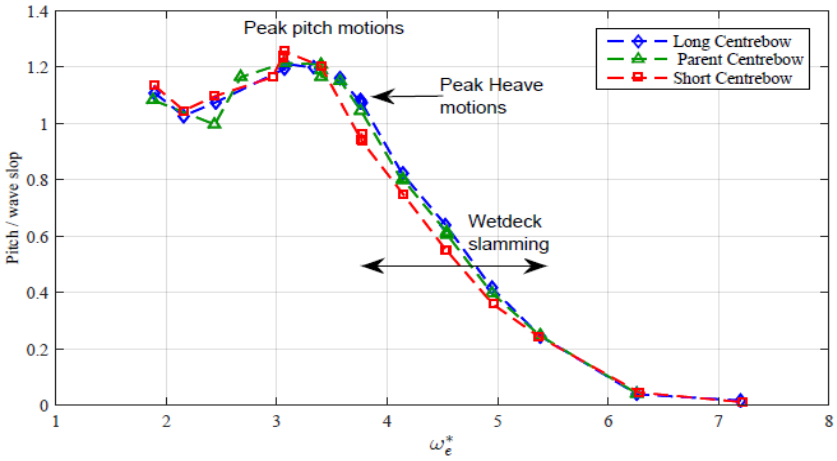

Figure 12: Non-dimensional pitch response (RAO) for the three centre bow lengths in HSM02 ($H_w = 60$ mm, speed=1.53 m/s)

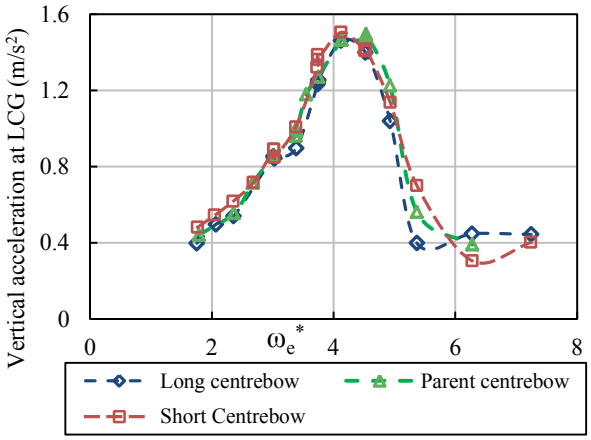

Figure 13: Accelerations measured at the LCG of the model for the three centre bow lengths in HSM02

Figure 13 shows the acceleration results at the LCG calculated from the two LVDT motion signals. The signals were low pass filtered with 4th order Butterworth with 5 Hz cut off frequency to remove the high frequency components of noise and structural vibrations. As seen, the peak LCG accelerations occurred around $\omega_e^* = 4.13$ which is higher than the heave and pitch peak frequency but a little less than peak slamming conditions. There is no significant difference between magnitudes of peak accelerations with the differing bow lengths.

Figure 14 shows the accelerations at a location 37% of LOA forward of LCG, corresponding to the forward end of the bridge at full scale, measured by a B&K accelerometer. Accelerations at this position are significantly greater than at the LCG due to the hull pitching motion. At $\omega_e^* = 4.13$ where peak accelerations are observed, it is evident that the larger centre bow volumes increased the accelerations at this more forward position. The results show that the long bow accelerations are around 7% higher compared to the vessel with the parent bow. Similarly, parent bow accelerations are 9% higher than the short bow. The reason for this difference between the accelerations

would be the variation in slam induced load severity in the forward bow areas of the vessel. To investigate the loads induced to the model, vertical bending moments are analysed in the next section.

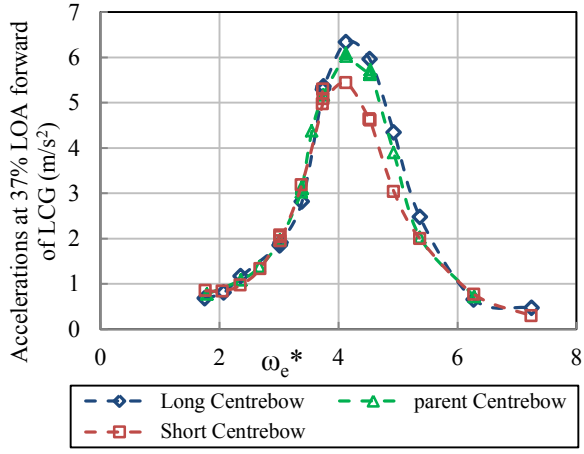

Figure 14: Acceleration measured (and filtered) at 37% LOA forward of LCG for the three centre bow lengths in HSM02 (H_w = 60 mm , speed=1.53 m/s)

5. VERTICAL BENDING MOMENTS (VBMs)

VBMs were derived from the strain gauges on the elastic links at the transverse cuts. The forward cut is at 1409 mm (56% of LOA) from the transom and the aft cut is located 820 mm (33% of LOA) from the transom. In the sagging situation VBM is considered positive and in the hogging VBM is negative and the VBM at each cut is the addition of the VBM from the starboard and port side elastic links.

Figure 15 shows sample time histories of the VBM recorded at the forward cut in (a) run 45 (ω_e^* = 4.13) and (b) run 37 (ω_e^* = 6.28) both with H_w = 60 mm and speed=1.53 m/s. In calm water and at zero speed, VBMs were first removed in each run to eliminate instrumentation bias signals before testing in waves. Figure 15(a) shows the global bending moments due to the encountered waves with only modest levels of whipping or bending vibration being evident. Figure 15(b) clearly shows the slam induced sharp VBM peaks and the consequent strong vibrational loading due to hull whipping. The peaks are visible after a peak slam sagging VBM and are followed by large whipping oscillations around the mean line.

Conducting Fast Fourier Transform analysis on the slam induced VBM signals revealed that the whipping vibratory response of the model to wave slam is at 12.82 Hz, somewhat lower than the impulse response at 14.7 Hz in calm water at zero speed. The whipping effects are significant and they are not fully damped by the time that the next slam is experienced. The average damping ratio of the VBMs for this run is 0.23, which is significantly greater than the value of 0.015 for the model in calm water and at zero speed. Full-scale slam decay coefficients calculated by Thomas (Thomas et al., 2008) on INCAT Hull 050 (96 m length) ranged between 0.05 and 0.4. This means that the model structural damping ratio is in a similar range to that of full-scale vessels. Figure 16 shows a sample strain gauge record from a full-scale keel plate on INCAT Hull 042 (86 m length) after being excited by a slam (Thomas, 2003). The comparison between the model raw data and full-scale data demonstrates the effectiveness of the model in replicating the dynamic behaviour of the full-scale vessel.

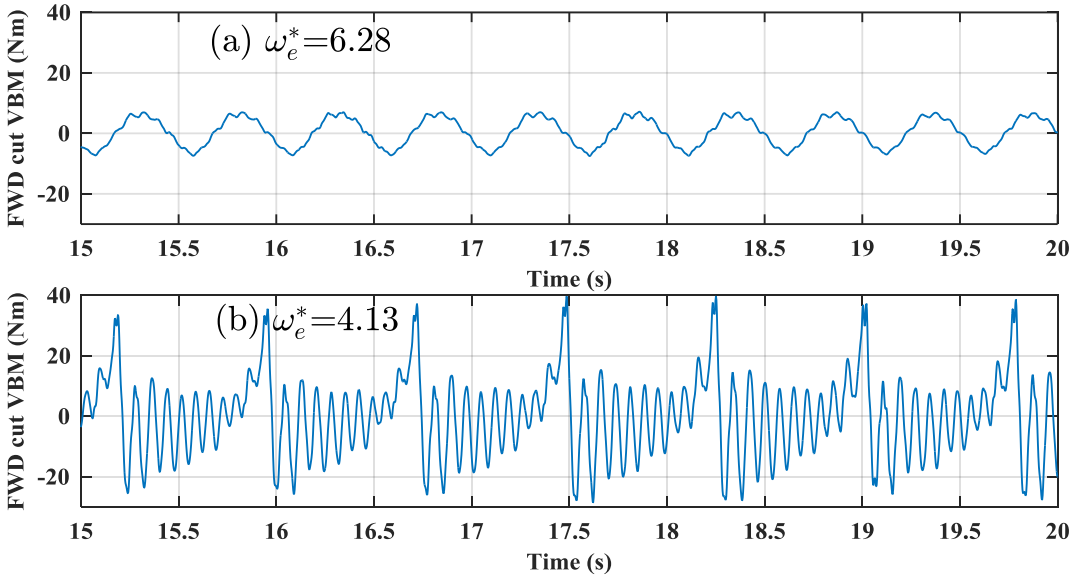

Figure 15: Sample recording VBM data of forward cut (56% LOA) for H_w = 60 mm, speed=1.53 m/s for (a) run 37 with ω_e^* = 6.28 and (b) run 45 with ω_e^* = 4.13

The whipping frequency is not an exact multiple of the slam or wave encounter frequency of course. Hence, each slam-induced VBM peak can vary as they are influenced by the slam load severity and also by the whipping effects from the previous slam. Observing such variations in VBM peak values (as seen in Figure 15(b)) demands presentation of the loads in a probabilistic manner to show the uncertainty involved. In a given environmental condition, both the distribution of load values and the extreme loads can be important.

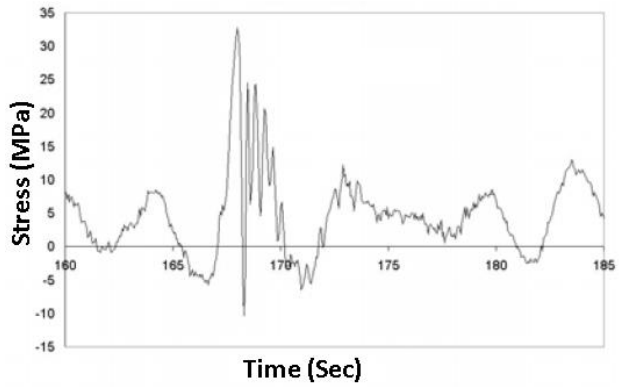

Figure 16: Keel plate stresses frame 24.5 of full-scale measurements on INCAT Hull042 catamaran (86 m length) (Thomas et al., 2008).

Depending on the encounter wave frequency, the number of regular wave load cycles observed in each towing tank run varied between 7 and 25 peaks. In the runs where slamming occurred the number of slams was between 12 and 20. To identify the distribution of peak values as an example, the results of aft cut sagging VBM peak values from four similar runs with $\omega_e^* = 4.53$ (the encounter frequency with the largest slam loads) in the parent centre bow configuration were analysed. Figure 16 shows the histogram of these VBM peak values where from the total of 78 peak values the mean is 38.48 Nm and the standard deviation is 2.79 Nm. It is seen that the samples are somewhat evenly distributed around the mean value and this suggests that a normal distribution can be assumed for the VBM values for a particular run.

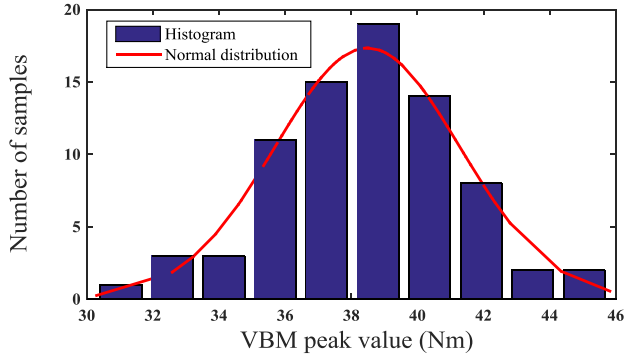

Figure 17: The histogram of slam induced VBM peak values for the forward cut during similar 4 runs (H_w = 60 mm, speed=1.53 m/s, $\omega_e^* = 4.53$). The mean is 38.48 Nm and standard deviation is 2.79.

To verify this assumption, a Kolmogorov–Smirnov test (Justel et al., 1997), a nonparametric test of the equality of continuous, one-dimensional probability) was performed on the data, which showed that with 98.7% confidence a normal distribution can be accepted for this distribution. Figure 18 shows the cumulative distribution function for the normal distribution and the sample data where good concurrence is observed.

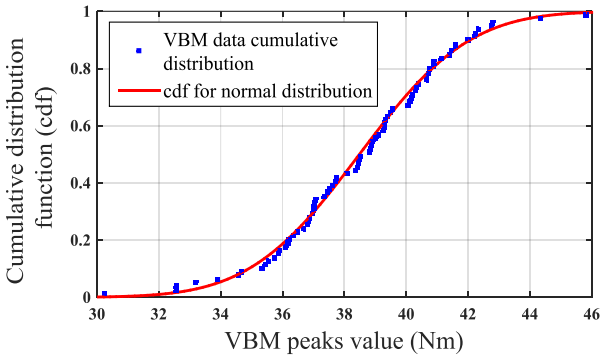

Figure 18: The cumulative distribution of the VBM peak values of parent centre bow during 4 similar runs compared to the normal distribution (H_w =60 mm, speed=1.53 m/s, $\omega_e^* = 4.53$)

The VBM values in hogging or sagging condition were calculated as the mean of the peak values in each encountered wave when the run was in steady wave conditions. The non-dimensional bending moment, VBM* is calculated by Equation (5),

$$VBM^* = \frac{VBM}{\rho g H_w \nabla} \qquad (5)$$

based on the method used by Colwell (Colwell et al., 1995), where ρ is the water density, H_w is the wave height and ∇ is the vessel displaced volume. Figures 19 and 20 show the measured peak bending moment in forward cut (56% of LOA) and aft cut (33% LOA) for the three centre bows with 95% confidence intervals as a function of the non-dimensional encounter frequency. As can be seen for high and low encounter wave frequencies the measured VBM results tend to zero and there is negligible difference between the three centre bows in those regions. In the frequency range of slamming ($3.7 \leq \omega_e^* \leq 5$) the VBM values increase and there is a clear difference between the responses of the three centre bows. Although there is not a sharp peak, the VBM due to slamming is close to a maximum when $4.13 \leq \omega_e^* \leq 4.53$.

The hogging VBMs are smaller than sagging VBMs in the frequency range of slamming. The hogging peaks are of course the consequence of the slam events which induced the preceding sagging peaks when the archways are filled up after a wet deck slam. The hogging moments arise as a combination of two effects: the commencement of whipping vibration and downward loads on the bow as

it moves upwards out of the water after a slam event, the latter being associated with added mass of the bow whilst in the water.

Figures 19 and 20 also show that the average VBM peak value for the long centre bow was 52% and 40% higher than the short centre bow at the forward and aft cuts respectively. This difference can be attributed to higher total slam forces imposed on the longer centre bow compared to the shorter centre bow.

Figure 21 show the non-dimensional VBM recorded in severe slamming conditions at the forward and aft cuts as a function of Centre bow Length Ratio (CLR) for different non-dimensional encounter wave frequencies. As can be seen, the VBM peaks in slamming conditions increase monotonically with the centre bow length ratio. This is an important trend, which shows the slam-induced loads on the structure increase linearly with the centre bow length.

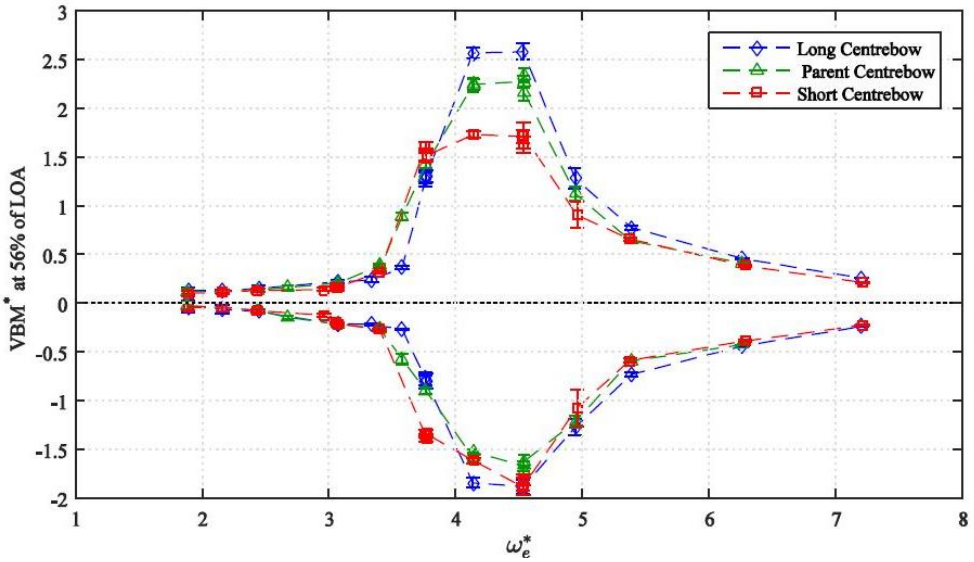

Figure 19**:** The non-dimensional forward cut (56% LOA) peak vertical bending moment ($VBM*$) for the three centre bow lengths ($VBM^* = \frac{VBM}{\rho g H_w \nabla}$)

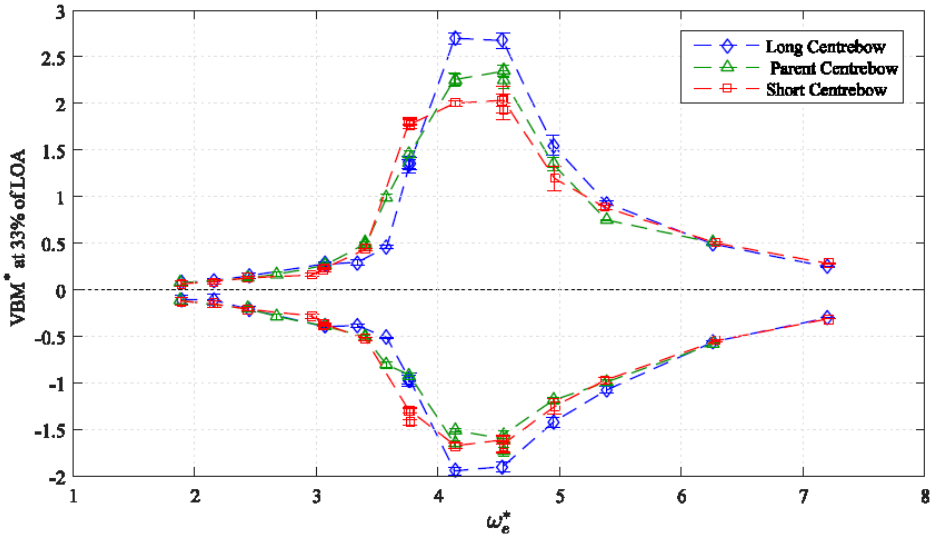

Figure 20**:** The non-dimensional aft cut (33% LOA) vertical bending moment (VBM^*) for the three centre bow lengths ($VBM^* = \frac{VBM}{\rho g H_w \nabla}$)

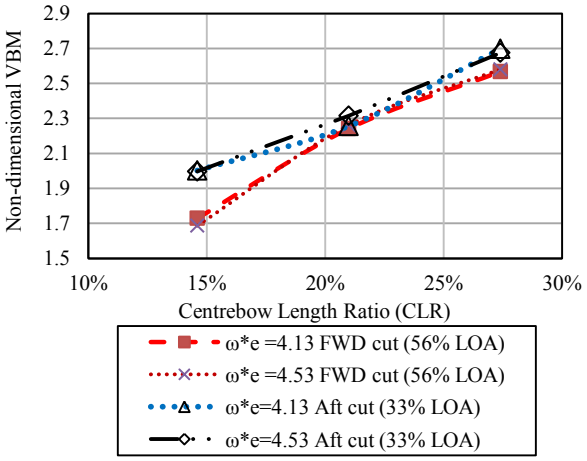

Figure 21: Non-dimensional vertical bending moment for varying centre bow length at two locations along the model

In summary, for the tested condition (equivalent to 20 knots forward speed and 2.68m waves) it has been seen that the heave results showed up to 17% difference between the three bow lengths, whereas the pitch results varied by only about 5%. The bow accelerations were about 25% less for the shorter centre bow than the longer centre bow under slamming conditions. The VBMs were also significantly lower for the short centre bow and increased monotonically with the centre bow length. The main reason for the lower slamming loads with the short centre bow is the lower volume of water being constrained under the wetdeck within the archways as most of the water displaced by the shorter bow can be displaced outwards in a sideways direction over the projecting demi-hull bows in the unconfined areas of the bow. Although this sea condition and speed does show a representative example of slamming for the WPC design, other speeds and wave heights need to be examined to establish a more thorough conclusion.

6. CONCLUSIONS

Measurement of motions and loads for each of the three models of varying centre bow length was undertaken successfully in regular waves of 60 mm height (2.68m full-scale) and at 1.53 m/s speed (20 knots full-scale) at different wave encounter frequencies. The results can be summarised as following:

- The heave motions of the vessel showed a maximum at dimensionless encounter frequency $\omega_e^* = 3.7$. The peak heave of the short centre bow was higher than the parent, and the parent centre bow was higher than the long centre bow. At other frequencies, the difference in the heave RAO between the centre bows was much reduced.
- The maximum peak of the pitch response of the vessel was in the range $3 \leq \omega_e^* \leq 3.5$. Only a small difference was observed between the peak values of the three model configurations. However, a slight shift of the frequency of maximum pitch for the short centre bow toward lower frequencies was observed. The reason was likely due to the reduction in model hydrostatic stiffness with the short centre bow. The main difference in pitch response was in the frequency range of slamming ($4 \leq \omega_e^* \leq 5$) in which shorter centre bows had an average 5% less pitch compared to the longer centre bows.
- The peak LCG acceleration differences between the three bows were small at the LCG but at the forward end of the bridge position the accelerations showed about 20% differences between the three bows, being higher for the longer bows.
- The VBM peak values due to slamming increased as the centre bow length increased.

For the conditions tested, the shorter centre bow was shown to be more effective in slamming conditions by reducing both motions and loads. The reason is that with shorter centre bows the displaced water exits from the sides over the forward bows of the demi-hulls and does not become constrained under the archways. The larger slam forces arise for longer centre bows due to this constraint and induce larger upward pitch motions which can then intensify the slam condition further. This however, does not mean that the benefits of centre bow length reduction will increase if the centre bow is removed completely. Designers should note that although shorter centre bows may give less loads and motions in slamming conditions, the clear advantages of having a centre bow to prevent bow diving and the potentially more extreme nature of slams on a flat wet deck should not be overlooked. The main conclusion is that constraining the water between the centre bow and demi-hulls should be minimised as much as possible. This conclusion leads to a recommendation for future work to assess experimentally more diverse hull forms in the bow region, such as moving the jaw (the point where the bow connects to the upper edge of the forward wave piercing demi hull) further aft. However, due to the nonlinearity of the vessel motions with respect to the wave height it is difficult to extrapolate the results observed in the present tests to higher wave heights and for different wet deck clearances. Therefore more extensive testing in large wave height and higher speed conditions with variable wet deck clearances is a priority for future work.

7. ACKNOWLEDGMENTS

The authors would like to acknowledge the Australian Research Council Linkage Grant provided to collaboration between University of Tasmania and INCAT Tasmania. The authors would also like to acknowledge Stuart Freizer for his contribution into the development of new hull forms and Babak Shabani and

Mohammadreza Javanmardi for their assistance in the test programme and drafting the paper.

8. REFERENCES

1. AMIN, W., DAVIS, M. R. & THOMAS, G. A. 2008. *Evaluation of finite element analysis as a tool to predict sea loads with the aid of trials data*. 8th Symposium on High Speed Marine Vehicles (HSMV 2008). Naples,Italy.
2. BEREZNITSKI, A. 2001. *Slamming: The role of hydroelasticity*. International Shipbuilding Progress, 48**,** 333-351.
3. COLWELL, J., DATTA, I. & ROGERS, R. 1995. *Head seas slamming tests on a fast surface ship hull form series*. International Conference on Seakeeping and Weather. London, UK: RINA, London.
4. DAVIS, M. R. & WHELAN, J. R. 2007. *Computation of wet deck bow slam loads for catamaran arched cross sections*. Ocean Engineering, 34**,** 2265-2276.
5. DESSI, D., FAIELLA, E., GEISER, J., ALLEY, E. & DUKES, J. 2016. *Design, assessment and testing of a fast catamaran for FSI investigation*. In: KIM, K.-H. (ed.) 31st Symposium on Naval Hydrodynamics. Monterey, California, USA: Office of Naval Research.
6. FENTON, J. 1990. *Nonlinear wave theories*. The Sea, 9**,** 3-25.
7. FENTON, J. D. & MCKEE, W. D. 1990. *On calculating the lengths of water waves*. Coastal Engineering, 14**,** 499-513.
8. GE, C., FALTINSEN, O. M. & MOAN, T. 2005. *Global hydroelastic response of catamarans due to wetdeck slamming*. Journal of ship research, 49**,** 24-42.
9. HERMUNDSTAD, O. A. & MOAN, T. 2005. *Numerical and experimental analysis of bow flare slamming on a Ro–Ro vessel in regular oblique waves*. Journal of Marine Science and Technology, 10**,** 105-122.
10. ITTC 2014. ITTC – *Recommended Procedures and Guidelines*. *Seakeeping*. International towing Tank Conference.
11. JACOBI, G., THOMAS, G., DAVIS, M. & DAVIDSON, G. 2014. *An insight into the slamming behaviour of large high-speed catamarans through full-scale measurements*. Journal of Marine Science and Technology, 19**,** 15-32.
12. JUSTEL, A., PEÑA, D. & ZAMAR, R. 1997. *A multivariate Kolmogorov-Smirnov test of goodness of fit*. Statistics & Probability Letters, 35**,** 251-259.
13. KAPSENBERG, G. K. 2011. *Slamming of ships: where are we now?* Philos Transact A Math Phys Eng Sci, 369**,** 2892-919.
14. KAPSENBERG, G. K. & BRIZZOLARA, S. 1999. *Hydro-elastic effects of bow flare slamming on fast monohull*. 5th International Conference on Fast Sea Transportation, FAST'99. Seattle, Washington, USA.
15. LAVROFF, J., DAVIS, M., HOLLOWAY, D. & THOMAS, G. 2007. *The whipping vibratory response of a hydroelastic segmented catamaran model*. 9th International Conference on Fast Sea Transportation, FAST2007. Shanghai China.
16. LAVROFF, J., DAVIS, M. R., HOLLOWAY, D. S. & THOMAS, G. 2013. *Wave slamming loads on wave-piercer catamarans operating at high-speed determined by hydro-elastic segmented model experiments*. Marine Structures, 33**,** 120-142.
17. LLOYD, A. R. J. M. 1989. *Seakeeping: Ship Behaviour in Rough Weather,* Chichester, Ellis Horwood Limited.
18. MATSUBARA, S. 2011. *Ship motions and wave induced loads on high speed catamarans*. PhD thesis, University of Tasmania.
19. SWIDAN, A. 2016. *Catamaran wetdeck slamming: a numerical and experimental investigation*. PhD, The University of Tasmania.
20. SWIDAN, A., THOMAS, G., PENESIS, I., RANMUTHUGALA, D., AMIN, W., ALLEN, T. & BATTLEY, M. 2017. *Wetdeck slamming loads on a developed catamaran hullform – experimental investigation*. Ships and Offshore Structures, 12**,** 653-661.
21. SWIDAN, A., THOMAS, G., RANMUTHUGALA, D., AMIN, W., PENESIS, I., ALLEN, T. & BATTLEY, M. 2016. *Experimental drop test investigation into wetdeck slamming loads on a generic catamaran hullform*. Ocean Engineering, 117**,** 143-153.
22. THOMAS, G. 2003. *Wave slam response of large high speed catamarans*. PhD Thesis, University of Tasmania.
23. THOMAS, G., DAVIS, M., HOLLOWAY, D. & ROBERTS, T. 2003. *Transient dynamic slam response of large high speed catamarans*. Proceedings of FAST 2003, The 7th International Conference on Fast Sea Transportation, 7th-10th October 2003a Ischia (Italy). B1-B8.
24. THOMAS, G., DAVIS, M., HOLLOWAY, D. & ROBERTS, T. 2008. *The vibratory damping of large high-speed catamarans*. Marine Structures, 21**,** 1-22.
25. THOMAS, G., MATSUBARA, S., DAVIS, M., FRENCH, B., LAVROFF, J. & AMIN, W. 2012. *Lessons learnt through design, construction and testing of hydroelastic model for determining motions, loads and slamming behaiviour in sever sea states*. In: TAKAGI, K. & OGAWA,

Y. (eds.) Hydroelasticity in Marine Technology. Tokyo, Japan: The University of Tokyo.

26. THOMAS, G., WINKLER, S., DAVIS, M., HOLLOWAY, D., MATSUBARA, S., LAVROFF, J. & FRENCH, B. 2010. *Slam events of high-speed catamarans in irregular waves*. Journal of Marine Science and Technology, 16**,** 8-21.
27. THOMAS, G. A., DAVIS, M. R., HOLLOWAY, D., WATSON, N. L. & ROBERTS, T. 2003b. *Slamming response of a large high-speed wave-piercer catamaran*. Marine Technology and SNAME News, 40**,** 126-140.
28. WHELAN, J. R. 2004. *Wetdeck slamming of high-speed catamarans with a centrebow*. PhD Thesis, University of Tasmania.

